



Topographic Maps and Local Contrast Changes in Natural Images

VICENT CASELLES

Department of Mathematics and Informatics, University of Illes Balears, 07071 Palma de Mallorca, Spain
dmivca0@ps.uib.es

BARTOMEU COLL

Department of Mathematics and Informatics, University of Illes Balears, 07071 Palma de Mallorca, Spain
dmitcv0@ps.uib.es

JEAN-MICHEL MOREL

CMLA, ENS. Cachan, 61 Av. du Président Wilson, Cachan, France
Jean-Michel.Morel@cmla.ens-cachan.fr

Received January 5, 1996; Revised December -, 1997; Accepted September 15, 1998

Abstract. We call “natural” image any photograph of an outdoor or indoor scene taken by a standard camera. We discuss the physical generation process of natural images as a combination of occlusions, transparencies and contrast changes. This description fits to the phenomenological description of Gaetano Kanizsa according to which visual perception tends to remain stable with respect to these basic operations. We define a contrast invariant presentation of the digital image, the topographic map, where the subjacent occlusion-transparency structure is put into evidence by the interplay of level lines. We prove that each topographic map represents a class of images invariant with respect to local contrast changes. Several visualization strategies of the topographic map are proposed and implemented and mathematical arguments are developed to establish stability properties of the topographic map under digitization.

Keywords: topographic map, mathematical morphology, level set, junctions, contrast changes, digitization

1. Introduction

What are the basic, computable elements from which the analysis of any natural image could start? The edges, that is, the discontinuity lines in an image have been and still are frequently considered as the basic objects in images, the “atoms” on which most Computer Vision algorithms can be built (Marr, 1981). There is no single definition for them, however. Many techniques from functional analysis have been proposed. A review of the variational approaches can be found in (Morel and Solimini, 1994), where it is argued that,

knowingly or not, all edge detection methods are variational. To make short a long story, let us recall that a digital image is modelled as a real function $u(x)$, where x represents an arbitrary point of the plane and $u(x)$ denotes the grey-level at x . In practice, an image has discontinuities everywhere, so that some selection process of the “true” discontinuities (or edges) must be defined. One way to do the selection of the “right” discontinuities is to smooth previously the image by some convolution or diffusion process, after which edges are detected as local extrema of the gradient magnitude in the gradient direction (Marr, 1981;

Canny, 1986). Then these points must be connected to form curves. Another way to do this selection is to have an a priori model of the image, describing which kind of discontinuities are expected (and which kind of regularity). These expectations are translated into an energy functional $E(u, u_0)$ where u_0 is the original digital image, and u an arbitrary element of an admissible class of interpretable images (e.g. with smooth regions and smooth discontinuity lines). Such a model for images is to impose (as proposed in (Rudin, 1987)) to u that it belongs to BV (space of functions with bounded variation), so that, by a classical theorem in geometric measure theory, the discontinuity set is rectifiable, i.e., contained in a countable union of curves with finite length.

Our aim here is to propose a different definition of the basic curve structure of an image, the topographic map, that is, a complete description of the image by its levels lines and junctions of level lines. By a complete description of the image, we mean a description from which the image can be fully reconstructed. Our argumentation is as follows. First, we describe the main physical accidents of the generation process of natural, “real world” images. Then we deduce from invariance requirements with respect to the accidents what information is left: the level lines. In two words, the main reason why level lines appear central is that they contain all of the image information invariant with respect to local contrast changes. The main operations in the generation process are *occlusion and transparency*: they generate junctions of level lines and leave as only invariants the pieces of level lines joining them. As a result, we propose a computational model for singularities of Kanizsa (1979, 1991) theories: T-junctions. Further technological applications have been developed since the first version of this paper and will be discussed at the end of this paper. At the computational level, the algorithm computing the topographic map of digital images is extremely simple, since it is based on the computation of level lines as the topological boundaries of level sets (which are computed by a simple thresholding!).

As a first algorithm analysing the topographic map, we propose a digital junction detector which works without previous smoothing of the image. Among works which have considered algorithms for the detection of T-junctions in images, we would like to mention (Alison Noble, 1992), which proposes a rather successful mix of edge detection techniques and mathematical morphology. Other attempts to obtain T-junctions

from a previous edge detection step are proposed in (Deriche and Giraudon, 1993; Lindeberg, 1994; Nitzberg and Mumford, 1990). These methods are all based on a Gaussian-like convolution followed by an analysis of edges and are not invariant with respect to contrast changes. Now, as explained in (Deriche and Giraudon, 1993; Alvarez and Morales, 1994), the T-junctions detection methods using a previous smoothing of the image tend to alter the junctions and let the edges vanish precisely where they are needed: in a neighborhood of the junction. So such methods necessitate, after the edge detection, a subsequent following up of the edges to restore the junctions. In the same way as we do, Romeny et al. (1991) consider geometric properties of isophotes and in particular their invariance under nonlinear intensity transformation. They propose to use the gradient of isophotes curvature as a good candidate for a T-junction detector. This method requires a previous smoothing of the image by heat equation and the computation of third order derivatives. Brunnström et al. (1992) considered how junction detection and classification can be performed in an active visual system. Beymer (1991) analysed junctions defined as the intersection points of three or more regions in an image, which is basically what we also propose but without the need of a previous gradient computation. Deriche and Blaszk (1993) proposed efficient models associated to edges, corners and junctions to extract and characterize these features directly from the image. In contrast, we do not push the characterization or classification of T-junctions or others, but argue that they might be selected among the more general kind of junctions yielded without any preprocessing by the topographic map. In particular, we think that level lines and their junctions can be a better starting point than edges in the clever non local grouping algorithms developed by Heitger and von der Heydt (1993) and Nitzberg-Mumford (1990) and in the structural analyses performed by Malik (1987) and Leclerc-Zucker (1987). In (Alvarez and Morales, 1994) is presented a rigorous theory for detecting corners. Now, the proposition made therein, that junctions can be detected as the coincidence of several corners, does not take advantage of the topological difference between corners and junctions. Junctions, as meeting points of level lines, are in fact easier to detect than corners.

Our plan is as follows. In Section 2 we shall sketch the process of image formation and show how this process leads to invariance requirements for the image

operators. We shall be particularly interested in the singularities which are inherent to the image formation process (T-junctions). In Section 3, we deduce which are the largest invariant objects in an image, containing the basic information and being a full representation of it. They constitute the basic structure of the image: the topographic map. In Section 4, we formally define the topographic map and prove it to be the invariant structure of an image under local contrast changes and we display some examples. In Section 5 we analyze the stability properties of the topographic map under digitization. Section 6 is devoted to the effective computation of level lines and junctions of the image and to first experiments. We then discuss different visualisation strategies for the topographic map. We finish with a discussion in Section 7.

2. How Natural Images are Generated: Occlusion and Transparency as Basic Operations

We shall, following the psychologist and gestaltist Gaetano Kanizsa, define two basic operations for image generation: *occlusion and transparency*. In the same way as in acoustics, where the basic operation, the superposition of transient waves, is interpreted as an addition of functions in a Hilbert space, *we shall interpret occlusion and transparency as basic operations on images considered as functions $u(x)$ defined on the plane*.

The description of image generation which follows is intentionally sketchy, since our aim is to arrive at invariance requirements from the most straightforward accidents of image generation. Our description of image generation will at first neglect the digitization effects (that is, convolution and sampling). Later, in Section 5, we shall see how, assuming a simplified model for image formation with a diffraction limited optical system, the grey level quantization involved in the digitization process comes to our help to maintain the basic geometric structure of the scene which is distorted by the convolution imposed by the finite aperture of the optical system.

2.1. Occlusion

As common knowledge indicates, we only see parts of the objects in front of us because they occlude each other. Let us formalize the basic operation of adding a new object in front of the scene. Given an object \tilde{A} in

front of the camera, we call A the region of the image plane onto which it is projected by the camera. We call u_A the grey level image of \tilde{A} thus generated, which is defined in the plane region A . Assuming now that the object \tilde{A} is added in a real scene \tilde{R} of the world whose image was v , we observe a new image which depends upon which part of \tilde{A} is in front of objects of \tilde{R} , and which part in back. Assuming that \tilde{A} occludes objects of \tilde{R} and is occluded by no object of \tilde{R} , we get a new image $u_{\tilde{R}\cup\tilde{A}}$ defined by

$$\begin{aligned} u_{\tilde{R}\cup\tilde{A}} &= u_A & \text{in } A \\ u_{\tilde{R}\cup\tilde{A}} &= v & \text{in } \mathbb{R}^2 \setminus A. \end{aligned} \quad (1)$$

Of course, we do not take into account in this basic model the fact that objects in \tilde{R} may intercept light falling on \tilde{A} , and conversely. In other words, we have omitted the shadowing effects, which will now be considered.

2.2. Transparency (or Shadowing)

Let us assume first that one of the light sources is a point in euclidean space, and that an object \tilde{A} is interposed between a scene \tilde{R} whose image is v and this light source. We call \tilde{S} the shadow spot of \tilde{A} and S the region it occupies in the image plane. The resulting image u is defined by

$$\begin{aligned} u_{\tilde{R},\tilde{S},g} &= v & \text{in } \mathbb{R}^2 \setminus S \\ u_{\tilde{R},\tilde{S},g} &= g(v) & \text{in } S. \end{aligned} \quad (2)$$

Here, g denotes a contrast change function due to the shadowing, which is assumed to be uniform in \tilde{S} . Clearly, we must have $g(s) \leq s$, because the brightness decreases inside a shadow, but we do not know in general how g looks. The only assumption for introducing g is that points with equal grey level s before shadowing get a new, but the same, grey level $g(s)$ after shadowing. Of course, this model is not true on the boundary of the shadow, which can be blurry because of diffraction effects or because the light source is not really reducible to a point. Another problem is that g in fact depends upon the kind of physical surface which is shadowed so that it may well be different on each one of the shadowed objects. This is no real restriction, since this only means that the shadow spot S must be divided into as many regions as shadowed objects in the scene; we only need to iterate the application of the preceding model accordingly.

A variant of the shadowing effect which has been discussed in perception psychology by Gaetano Kanizsa (1979) is, following Fuchs (1923), *transparency*. In the transparency phenomenon, a transparent homogeneous object \tilde{S} (in glass for instance) is interposed between part of the scene and the observer. Since \tilde{S} intercepts part of the light sent by the scene, we still get a relation like (2), so that transparency and shadowing are equivalent from the image processing viewpoint. If transparency (or shadowing) occurs uniformly on the whole scene, the relations (2) reduce to

$$u_g = g(v), \quad (3)$$

which means that the grey-level scale of the image is altered by a nondecreasing contrast change function g .

2.3. Requirements for Image Analysis Operators

Of course, when we look at an image, we do not know a priori what are the physical objects which have left a visual trace in it. We know, however, that the operations having led to the actual image may include formulas (1, 2). Thus, any processing of the image should avoid to destroy the image structure resulting from (1, 2). *The identity and shape of objects must be recovered from the image by means which should be stable with respect to those operations.* Thus, our physical simple model for image generation already imposes that image analysis operations should be invariant with respect to any contrast change, a requirement proposed by Matheron (1975). We shall say that an operation T on an image u is *contrast invariant* if

$$T(g(u)) = g(T(u)) \quad (4)$$

for any nondecreasing contrast change g (classical examples of contrast invariant operators are erosion, dilation, opening and closing).

To further support the previous conclusion, we remark that most light sensors have a nonlinear behavior and, even worse, have a finite range. Whenever light is too strong (or too weak), saturation of the sensors occurs (see Fig. 1). The contrast changes are not only caused by the sensors but also due to the changes of the light intensity and the same objects. In other words, not only there exists a global contrast change when illumination intensity changes but also a contrast change conditioned by the objects in the scene. This is one of the informations provided by formulas (1, 2). We shall

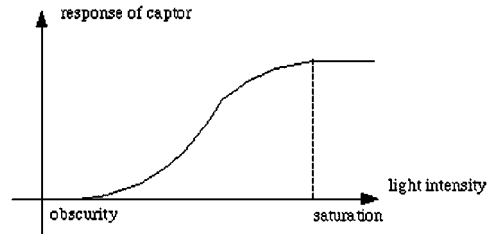


Figure 1. Nonlinear response of sensors.

formalize this notion as local contrast change invariance in Section 4, Definition 5.

By the contrast invariance requirement in computer vision, we by no means suggest that human vision is insensitive to contrast: It is plain that we do not see the same objects when we change the contrast of an image (see e.g. (Illueca, 1995)). In fact, the contrast invariance requirement is nothing but a theory of information requirement in the computational use of digital images: we assert that even though some level lines can be below our range of sensitivity, they contain useful geometric information. Such information is typically recovered by a viewer by adjusting the contrast of the image he is looking at. In contrast, the fact that an “edge” have a strength of say 10 or 30 does not change at all its geometric contents. Wertheimer (1923) stated this remark, the irrelevance of grey level, as a basic principle of Gestalt theory.

In the same way, rotation invariance is generally assumed in Computer Vision tasks, in contrast to our well known preference for vertical and horizontal lines and to the fact that our interpretation of objects is influenced by our recognition and is certainly not rotationally invariant.

The evidence of contrast invariance in some tasks of human shape recognition is only indirect, but strong. Indeed, Julesz texton theory proposes extrema of curvature (corners, terminators in his terminology) as well as their orientation as clues to texture detection. In the same way, Attneave’s theory of human shape recognition also relies on extrema of curvature and inflexion points. Now, it is noticeable that both orientation and curvature are invariant with respect to global and even local contrast changes in the sense we have defined in this paper. Indeed, the orientation is given by a vector tangent to the isophote and is not altered by a contrast change. In the same way, curvature is computed as the curvature of the level lines and does not depend on local contrast.

3. The Basic Structure for Image Analysis

We call *basic objects* a class of mathematical objects, simpler to handle than the whole image, but into which any image can be decomposed and from which it can be reconstructed. Two classical examples of image decompositions are

- Additive decompositions into simple waves: Basic objects of Fourier analysis are cosine and sine functions, basic objects of Wavelet analysis are wavelets or wavelet packets, basic objects of Gabor analysis are gaussian modulated sines and cosines. In all of these cases the decomposition is an additive one and we have argued against it as not adapted to the structure of images, except for restoration processes. Indeed, operations leading to the construction of real world images are strongly nonlinear and the simplest of them, the contrast change, does not preserve additive decompositions. If $u = u_1 + u_2$, then it is not true that $g(u) = g(u_1) + g(u_2)$ if the contrast change g is nonlinear. This objection does not apply to image compression, because in compression tasks, the fine scale structure of the image dominates and this structure is linear: By Shannon sampling theory, the image must be the result of a fine convolution, so that, at fine scale, the image indeed is a sum of waves.
- Next, we have the representation of the image by a *segmentation*, that is, a decomposition of the image into homogeneous regions separated by boundaries, or “edges”. The notion of edge as a discontinuity of the image $u(x)$ is not against the contrast invariant axiom. Indeed, if g is any continuous and increasing contrast change and u has a discontinuity at x_0 , then $g(u)$ is also discontinuous at x_0 , and conversely. The notion of discontinuity does not impose a minimum strength on the jump but, in practice, one cannot compute them without fixing the strength of contrast on the edges, typically a uniform value for the whole image. This criterion is not invariant with respect to contrast changes. Indeed $\nabla g(u) = g'(u)\nabla u$ and $g'(u)$ is close to zero when the image is close to obscurity or saturation. Moreover, classical edge detection basically consists of a convolution of u with a kernel k , followed by a differential edge detector. Now, clearly, if g is nonlinear, $k \times (g(u)) \neq g(k \times u)$.

Mathematical morphology offers an alternative: to decompose an image u into its binary shadows (or level sets), that is, we set $X_\lambda u = \{x \in \mathbb{R}^2: u(x) \geq \lambda\}$. The

sets $X_\lambda u$, or simply X_λ , are called *level sets* of u . An image can be reconstructed from its level sets by the formula

$$u(\mathbf{x}) = \sup\{\lambda, u(\mathbf{x}) \geq \lambda\} = \sup\{\lambda, \mathbf{x} \in X_\lambda u\}. \quad (5)$$

The decomposition is therefore nonlinear, and reduces the image to a family of plane sets $\{X_\lambda\}$. Obviously, if we transform an image u into $g(u(x))$, where g is an increasing continuous function (understood as a contrast change), then it is easily seen that the set of level sets of $g(u(x))$ is equal to the set of level sets of u . A stronger invariance is even possible if we note that by formulas (1, 2) the contrast change can affect only the connected parts of the level sets of u . This contrast invariance will be precisely defined in the next section. Let us begin by defining the topographic map of an image.

Let Ω be a domain in \mathbb{R}^2 . Let $u: \Omega \rightarrow \mathbb{R}$ be an image, i.e., a bounded measurable function.

Definition 1. Given an image u , we call upper level set of u any set of the form $[u \geq \lambda]$ where $\lambda \in \mathbb{R}$.

Definition 2. (Choquet, 1966) Let X be a topological space. We say that X is connected if it cannot be written as the union of two nonempty closed (open) disjoint sets. A subset C of X is called a connected component if C is a maximal connected subset of X , i.e., C is connected and for any connected subset C_1 of X such that $C \subseteq C_1$, then $C_1 = C$.

Definition 3. The upper topographic map of an image is the family of the connected components of the level sets of u , $[u \geq \lambda]$, $\lambda \in \mathbb{R}$.

Note that, by (5), the upper topographic map associated with u uniquely determines the function u . We could have also used the lower level sets of u , $[u \leq \lambda]$.

We call *level lines* of u the boundaries of the upper level sets of u . If we assume that we can determine the level sets of u from their boundary level lines, then we shall refer to the topographic map of u as the family of level lines of u . This is the case if our image is such that, for each level set $[u \geq \lambda]$, $\lambda \in \mathbb{R}$ the boundary $\partial[u \geq \lambda]$ is made of a finite or countable union of closed Jordan curves. Then the oriented level lines perfectly define level sets, and, hence also the function u . Recall that a continuous curve is called a Jordan curve if it has no selfintersection, except possibly at its endpoints (Examples: a circle, a segment, a parabola).

This restricts our functional model for continuous images but does not represent any restriction for discrete or digital images. Indeed, in the discrete framework (or in any continuous interpolation framework for images), we can associate with each level set a unique finite set of oriented Jordan curves which define its boundary and, conversely, the level set is uniquely defined from those Jordan curves. We shall call them *level curves of the image*. In the following, we assume that these level curves exist, be it because the image is discrete or, e.g., in an adequate function space.

Definition 4. If u belongs to a function space, such that each connected component of a level set is bounded by a countable or finite number of oriented Jordan curves, we call topographic map the family of these Jordan curves.

Remark. When in the following we display the topographic map, we only display the Jordan curves, without specifying their level λ or orientation. Now, in order to ensure reconstruction of u , we of course need this information.

If we assume that the level sets are closed Caccioppoli subsets of \mathbb{R}^2 , that is, closed sets whose boundary has finite length, then its essential boundary is a countable or finite union of closed Jordan curves and, possibly, a set of null H^1 Hausdorff measure (see (Caselles and Morel, —)). In this case, we can describe the connected components of level sets by their boundary (see (Caselles and Morel, —)). This is an interesting case, since it covers the case of functions of bounded variation (or simply, BV functions) which have been frequently used as functional image models for purposes of denoising, edge detection, etc. (Rudin et al., 1992). If u is a function of bounded variation, $u \in BV(\Omega)$, then almost all level sets $[u \geq \lambda]$ are closed Caccioppoli sets (Evans and Gariepy, 1992). Then, the topographic map of u can be described in terms of the level lines of u and Formula (5) holds as well.

Two objections. Before starting with the mathematical model, let us discuss two serious objections which were raised by auditors and readers of a preliminary version of the present paper. The first is concerned by “shape from shading” models. Human performance in recovering shape from shading has been demonstrated in phenomenological rigorous experiences. Now, if the image is known up to a contrast change, then there is no way of recovering the 3D shapes from a single

view by the “shape from shading equation”. Contrast invariance is nonetheless a sound assumption when we look at a photograph of, say, a statue. In that case, we ignore lighting and photographing conditions. Thus, the reconstruction of the 3D shape from a photograph is in theory impossible without some further information. Archeologists know this well, since they are not contented with photographs of objects found, but ask for a good conventional drawing. Lab. phenomenological experiments are a different story, since the subject is placed in known lighting conditions, so that the contrast invariance assumption is not valid anymore.

Another objection of a different kind is whether level lines can exist for textured image and yield a useful information. The answer is definitely yes. No matter how complicated the patterns of the level lines may look, they reflect the structure of the texture. We have commented right above that level lines of a digital image can *always* be computed (see e.g. Fig. 6.3 for a detail of a textured image.) Texture classification by the study of “granularity” is nothing but the exploration of the structure of small level sets, the boundary of which are small level lines (Serra, 1982).

4. Invariance Properties of the Upper Topographic Map

We now prove that the topographic map is a contrast invariant description of an image. We work in the continuous framework but all we shall say is obviously true for digital images. Let Ω be a domain of the plane (e.g., a rectangle). Given an image $u: \Omega \rightarrow \mathbb{R}$, $\lambda \in \mathbb{R}$ and $x \in [u \geq \lambda]$, we shall denote by $cc([u \geq \lambda], x)$ the connected component of $[u \geq \lambda]$ in Ω containing x .

Definition 5. We say that a multivalued map $h: \Omega \times \mathbb{R} \rightarrow \mathcal{P}(\mathbb{R})$ is a monotone multifunction if

(MM1) $h(x, \lambda)$ is an interval of \mathbb{R} for any $x \in \Omega$ and $\lambda \in \mathbb{R}$.

Let $h^-(., \lambda) = \inf\{\mu: \mu \in h(x, \lambda)\}$, $h^+(., \lambda) = \sup\{\mu: \mu \in h(x, \lambda)\}$.

(MM2) If $\lambda > \mu$, then either $h(x, \lambda) = h(x, \mu)$ or $h^+(., \mu) \leq h^-(., \lambda)$.

(MM3) $\cup_{\lambda \in \mathbb{R}} h(x, \lambda)$ is an interval of \mathbb{R} .

Definition 6. Let $u: \Omega \rightarrow [a, b]$ be a given image and let $\{X_\lambda: \lambda \in [a, b]\}$ be the family of its level sets. We shall say that a multivalued mapping $h: \Omega \times \mathbb{R} \rightarrow \mathcal{P}(\mathbb{R})$ is a local contrast change for u if

- (H1) h is a monotone multifunction such that for all $\lambda \in \mathbb{R}$, $h^-(\cdot, \lambda)$, $h^+(\cdot, \lambda)$ are measurable in Ω .
- (H2) If $u(x) < \lambda$ then $h^+(x, u(x)) = h^-(x, \lambda) < h^+(x, \lambda)$, $x \in \Omega$, $\lambda \in \mathbb{R}$.
- (H3) $h^+(x, \lambda) = h^+(y, \lambda)$ for all x, y belonging to the same connected component of $[u \geq \lambda]$, $\lambda \in \mathbb{R}$.
- (H4) Let $v(x) = h^+(x, u(x))$. If $y \in cc([v \geq \mu], x)$ where $\mu \in h(x, \lambda)$, $x \in \Omega$, $\lambda \in \mathbb{R}$, then $h(x, \lambda) = h(y, \lambda)$.

Definition 7. (Caselles et al., 1997) Let $u: \Omega \rightarrow [a, b]$ be an given image. We shall say that v is a local representative of u if there exists some local contrast change h such that $v(x) = h^+(x, u(x))$, $x \in \Omega$.

The next proposition states the fact, together with some other information, that local contrast changes preserve the upper topographic map and, therefore, also the topographic map.

Proposition 1. Let $u: \Omega \rightarrow [a, b]$ and let $v(x) = h^+(x, u(x))$, $x \in \Omega$, be a local representative of u . Then

- (i) $v(x) = \sup\{h^+(x, \lambda): x \in X_\lambda u\}$, $x \in \Omega$. We have that $x \in X_\lambda u$ if and only if $x \in X_{h(x, \lambda)} v$, $x \in \Omega$, $\lambda \in \mathbb{R}$.
- (ii) v is a measurable function.
- (iii) Let Γ (resp. Γ') be a connected component of $[v \geq \mu]$ (resp. $[u \geq \lambda]$) containing x and $\mu = h^+(x, \lambda)$. Then $\Gamma = \Gamma'$.
- (iv) For each connected component X of $[u \geq \lambda]$ there exists μ and a connected component Y of Y_μ such that $X = Y$ and conversely.

Let us state a converse statement to Proposition 1: If two images have the same upper topographic map then they are related by a local contrast change. Images can be considered as equivalence classes of functions, modulo local contrast changes. Proofs of Proposition 1 and Theorem 1 are given in the Appendix.

Theorem 1. Let $u, v: \mathbb{R}^n \rightarrow \mathbb{R}$ be two bounded measurable functions (images) whose upper level sets have, at most, countably many connected components. Let X_λ , respectively Y_λ , be the families of the level sets of u , respectively v . Given a level set X_λ (or Y_λ) and a point $x \in \mathbb{R}^n$, suppose that for each connected component X of X_λ there exists μ and a connected component Y of Y_μ such that $X = Y$ and a converse statement with

X_λ and Y_μ interchanged. Then there exists a local contrast change $g(x, \lambda)$ such that $v(x) = g^+(x, u(x))$.

In the next section, we shall study the stability of the topographic map during the process of image formation. It is a basic and stable tool which permits to manipulate the image (Masnou and Morel, 1997, 1998a). In (Caselles et al., 1998), a recovery by interpolation of level lines lost in the quantization process is investigated. An intuitive interpretation of the topographic map is contained in the following glossary:

- Connected components of level sets = Boolean union of physical objects.
- Level lines = Concatenations of pieces of boundaries of physical objects.
- Aligned junctions = Occlusion boundary.

Image 2.4 displays the topographic map associated to Image 2.2. We immediately see that it is a complicated object as far as visualization is concerned. In fact, this experiment shows that even an apparently simple image contains highly structured and abundant information. This information cannot be considered as “noise”. In Image 2.5 we show a partial view of the same topographic map by displaying only the level lines multiples of 10. Image 2.1 is an original image and Image 2.3 is its topographic map in the same way.

5. Stability of the Topographic Map

Given an image u , i.e., a bounded measurable function which we shall assume to be defined in \mathbb{R}^2 , the digitization process transforms it into a discrete version U defined on a lattice, say \mathbb{Z}^2 . What happened to the basic structure of u ? Have the level sets, level lines and junctions of U any connection to the corresponding facts at the continuous level?

We shall describe the digitization process $u \rightarrow U$ as the combination of the following operations:

1. Convolution with a filter G representing the point spread function of the optical apparatus used to acquire the image. We shall assume either that G is rotation invariant or that it has a square symmetry. Its size will be given in terms of the parameter r_1 described below.
2. Scanning modelled by a convolution (i.e., a moving average centered on the pixel) with a square pattern of the intensity over a region Q (the size of the



Image 2.1



Image 2.2

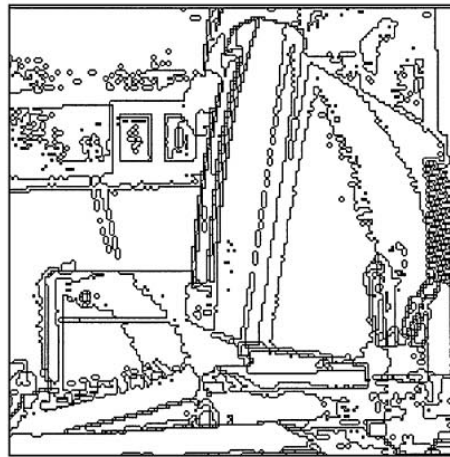


Image 2.3

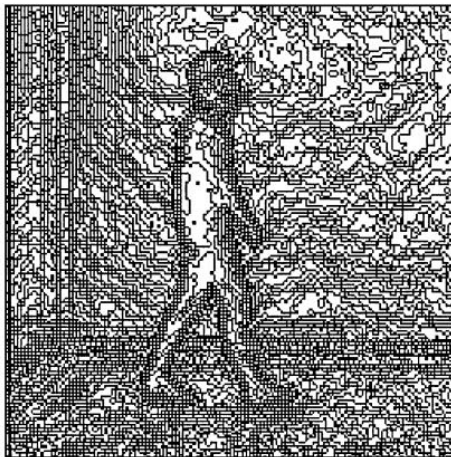


Image 2.4

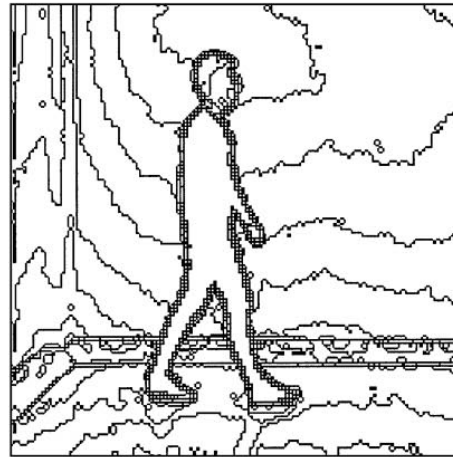


Image 2.5

Figure 2. Experiments on the topographic map. Image 2.1 and Image 2.2 are the original grey-level images. Image 2.3 shows the topographic map of Image 2.1, for levels which are multiples of 30. Image 2.4 displays the topographic map associated with Image 2.2, for all level lines multiples of 2. In Image 2.5, we can see the topographic map of Image 2.2 but showing only the level lines for levels which are multiples of 10.

pixel). This defines an operator $A_Q(u) = \chi_Q \times u$. Sampling will be modelled as the application of a Dirac comb S .

3. A uniform quantization operator, defined by $E(x) = k\Delta$ if $x \in](k - 1/2)\Delta, (k + 1/2)\Delta]$.

Hence, we may write $U = ESA_QG(u)$.

If the optical system is linear, translation invariant, and the light sources incoherent, then the physical image (the observed image intensity) at a point $x \in \mathbb{R}^2$ is

$$\tilde{u}(x) = \int_{\mathbb{R}^2} G(x - \xi)u(\xi)d\xi \quad (6)$$

where $G(x)$ is the incoherent point spread function and u is the intensity distribution of the radiation field. In the case of a circular aperture of diameter a in a narrow band incoherent light having center wavelength λ , the point-spread function is ((Castleman, 1996) chap. 15, (Hecht and Zajac, 1986), chap. 10)

$$G(x) = \left(2 \frac{J_1\left(\pi \frac{r}{r_0}\right)}{\pi \frac{r}{r_0}}\right)^2 \quad (7)$$

where $J_1(r)$ is the first order Bessel function of the first kind, r is the radial distance in the image plane and

$$r_0 = \frac{\lambda z}{a}, \quad (8)$$

z being the distance from the lens to the image plane. In case of a square aperture $[-a, a] \times [-b, b]$

$$G(x_1, x_2) = \frac{\sin^2\left(\pi \frac{x_1}{x_{01}}\right) \sin^2\left(\pi \frac{x_2}{x_{02}}\right)}{\left(\pi \frac{x_1}{x_{01}}\right)^2 \left(\pi \frac{x_2}{x_{02}}\right)^2} \quad (9)$$

where $x_{01} = \frac{\lambda z}{2a}$, $x_{02} = \frac{\lambda z}{2b}$ ((Castleman, 1996), chap. 15, (Hecht and Zajac, 1986), chap. 10).

In view of the previous discussion, we shall assume that the optical system is described by a convolution operator with a positive kernel G . Moreover, we shall assume that G is either rotationally invariant or has a separable representation like the one in (9). Let us finally discuss the size of the kernel and its relation with resolution of the imaging system ((Castleman, 1996), chap. 15, (Hecht and Zajac, 1986), chap. 10).

By resolution we mean the ability of the imaging system to reproduce the contrast of objects of various size. By contrast we mean the differences in intensity within an object or between the object and the surrounding background. According to the Rayleigh criterion

of resolution, two point sources can be resolved if they are separated, in the focal plane, by the distance $\delta = r_1$ where r_1 is the first zero of H , i.e., of the first order Bessel function, i.e., $r_1 = 1.22r_0$, $r_0 = \lambda z/a$ where z is the distance from the lens to the image plane and a is the diameter of the circular aperture. r_0 is called the radius of the Airy disk. A common way to specify the resolution of an imaging system is by the Rayleigh criterion. Notice that the diameter of the PSF is given, to a good approximation, by the Rayleigh distance ((Castleman, 1996), chap. 15, (Hecht and Zajac, 1986), chap. 10). The optical cutoff frequency in the image plane co-ordinate system of a camera with circular aperture of diameter a is

$$f_c = \frac{a}{\lambda z} = \frac{1}{r_0}$$

assuming narrow-band incoherent light with center wavelength λ . Let $F = 1/T$ be the highest spatial frequency of interest that is present in the image. Thus T is the period of the smallest detail of interest. As a rule of thumb, the diameter W of the scanning spot (the imaging system PSF) should be no larger than $T/2$, i.e.,

$$W \leq T/2$$

Thus the scanning spot would fit within one half-cycle of the highest frequency sine wave.

But independently of the frequencies present in the object, the imaging system constraints the maximum frequency to be no higher than the cutoff frequency f_c of the optical transfer function of the primary imaging lens. According to Nyquist criterion, we set the folding frequency, which is half of the sampling frequency, equal to f_c . Thus, the Nyquist criterion gives us $2f_c$ as sampling frequency. This places the pixel spacing at

$$\frac{1}{2f_c} = \frac{\lambda f\#}{2} = \frac{r_0}{2} = 0.5r_0$$

The Rayleigh criterion would give as sample spacing one-half of the Rayleigh distance. Then pixels will fall alternately upon and between (just resolvable) point sources separated by that distance in the image. In this case, point sources can be resolved in the digital image. The finest possible pixel spacing is thus ((Castleman, 1996), chap. 15)

$$0.61r_0.$$

According to the Rayleigh criterion, the folding frequency is at 82% of the OTF cutoff frequency f_c .

Aliasing is possible but it is unlikely to be significant in practice ((Castleman, 1996), chap. 15).

5.1. Digitization of Level Sets

Let us see the effect of the operators involved in the generation of physical images on the level sets of u . Taking realistic assumptions on the optical digital system, we shall give estimates in terms of pixels of the distance by which a level line can move in the digitization process. By $\mu_{\mathcal{L}}$ we denote the Lebesgue measure in \mathbb{R}^2 . For each $r > 0$, we shall denote by B_r the open ball of radius r centered at the origin of coordinates. Recall the definitions of erosion and dilation of a subset $X \subseteq \mathbb{R}^2$ by a structuring element $Y \subseteq \mathbb{R}^2$

$$\begin{aligned} X \ominus Y &= \{x \in \mathbb{R}^2 : x + Y \subseteq X\} \\ X \oplus Y &= \{x \in \mathbb{R}^2 : (x + Y) \cap X \neq \emptyset\}. \end{aligned}$$

Recall also that

$$\mathbb{R}^2 \setminus (X \ominus Y) = (\mathbb{R}^2 \setminus X) \oplus Y. \quad (10)$$

If $Y = B_\epsilon$, $\epsilon > 0$, then $X \oplus B_\epsilon = \{x \in \mathbb{R}^2 : d(x, X) < \epsilon\}$.

Let G be the convolution operator whose kernel $G(x)$ is a positive radially symmetric function such that

$$\int_{\mathbb{R}^2} G(x) dx = 1. \quad (11)$$

Let $\epsilon > 0$ and let $\eta > 0$ be such that

$$\int_{\mathbb{R}^2 \setminus B_\epsilon} G(x) dx = \eta. \quad (12)$$

Note that if G is of compact support contained in B_ϵ then we may take $\eta = 0$.

Lemma 1. *Let B be a measurable subset of \mathbb{R}^2 . Then,*

$$[G(\chi_B) > \eta] \subseteq B \oplus B_\epsilon \quad (13)$$

and

$$B \ominus B_\epsilon \subseteq [G(\chi_B) \geq 1 - \eta]. \quad (14)$$

Proof: If $x \notin B \oplus B_\epsilon$, then using (10) we have $(x + B_\epsilon) \cap B = \emptyset$. Then, setting $\chi_B(x) = 1$ if $x \in B$, $\chi_B(x) = 0$, otherwise,

$$\begin{aligned} G(\chi_B)(x) &= \int_{\mathbb{R}^2} G(x - y) \chi_B(y) dy \\ &= \int_{x + B_\epsilon} G(x - y) \chi_B(y) dy \\ &\quad + \int_{\mathbb{R}^2 \setminus (x + B_\epsilon)} G(x - y) \chi_B(y) dy \\ &= \int_{\mathbb{R}^2 \setminus (x + B_\epsilon)} G(x - y) \chi_B(y) dy \\ &\leq \int_{\mathbb{R}^2 \setminus B_\epsilon} G(z) dz = \eta \end{aligned}$$

Thus

$$\mathbb{R}^2 \setminus (B \oplus B_\epsilon) \subseteq [G(\chi_B) \leq \eta]$$

which gives (13).

If $x \in B \ominus B_\epsilon$, then $x + B_\epsilon \subseteq B$. Hence

$$\begin{aligned} G(\chi_B)(x) &= \int_{x + B_\epsilon} G(x - y) \chi_B(y) dy \\ &\quad + \int_{\mathbb{R}^2 \setminus (x + B_\epsilon)} G(x - y) \chi_B(y) dy \\ &\geq \int_{x + B_\epsilon} G(x - y) \chi_B(y) dy \\ &= \int_{x + B_\epsilon} G(y - x) dy \\ &= \int_{B_\epsilon} G(z) dz = 1 - \eta \end{aligned}$$

and (14) follows. \square

Consequence. Let u be an image and $\lambda' \in \mathbb{R}$. Then

$$G(u) \geq \lambda' G(\chi_{[u \geq \lambda']}) \geq \lambda'(1 - \eta) \chi_{[u \geq \lambda'] \oplus B_\epsilon}. \quad (15)$$

Hence $[u \geq \lambda'] \ominus B(0, \epsilon) \subseteq [G(u) \geq \lambda']$ where $\lambda = \lambda'(1 - \eta)$.

To prove a similar inclusion in the other direction, let $M = \sup\{|u(x)| : x \in \mathbb{R}^2\}$. Let us write $\xi = 1 - \eta$ which is a number close to 1. Observe that $M - u \geq (M - \lambda_0) \chi_{[u < \lambda_0]}$. Applying G to both sides and using that $G(1) = 1$ and (15) we get that

$$G(u) \leq M - (M - \lambda_0) \xi \chi_{[u < \lambda_0] \oplus B_\epsilon} \quad (16)$$

Now assume that $G(u)(x) > \lambda$, $\lambda < M$. Let λ_0 be such that

$$\frac{M - \lambda}{(M - \lambda_0)\xi} = 1, \quad (17)$$

that is, $\lambda_0 = M - \frac{M}{\xi} + \frac{\lambda}{\xi}$. Then, from (16), it follows that

$$\chi_{[u < \lambda_0] \oplus B_\epsilon}(x) < \frac{M - \lambda}{(M - \lambda_0)\xi} = 1.$$

Hence $\chi_{[u < \lambda_0] \oplus B_\epsilon}(x) = 0$, i.e., $x \in [u \geq \lambda_0] \oplus B_\epsilon$. We have shown that

$$[G(u) > \lambda] \subseteq [u \geq \lambda_0] \oplus B_\epsilon \quad (18)$$

where λ and λ_0 are related by (17). Obviously, if $\lambda = M$ and $G(u)(x) \geq M$ then also $u \geq M$. Thus we have proved the following Lemma.

Lemma 2.

(i) Let $\lambda' \in \mathbb{R}$, $\lambda = \lambda'(1 - \eta)$, $\lambda_0 = \lambda' - \frac{\eta M}{1 - \eta}$. Then

$$[u \geq \lambda'] \oplus B_\epsilon \subseteq [G(u) \geq \lambda] \quad (19)$$

and

$$[G(u) > \lambda] \subseteq [u \geq \lambda_0] \oplus B_\epsilon. \quad (20)$$

(ii) In a similar way, if $\lambda_0 < \lambda' - \frac{\eta M}{1 - \eta}$

$$[G(u) \geq \lambda] \subseteq [u \geq \lambda_0] \oplus B_\epsilon. \quad (21)$$

As a consequence, we obtain the following result.

Corollary 1. (Stability of step discontinuities) Let u be an image. We shall assume that $[u \geq \lambda]$ is a constant set D for all $\lambda \in [a, b]$. Let $k \geq 0$ and

$$\eta < \eta^* = \frac{b - a - k}{M + b - a}. \quad (22)$$

Then

$$\begin{aligned} D \oplus B_\epsilon &\subseteq [G(u) \geq b(1 - \eta)] \\ &\subseteq [G(u) > a(1 - \eta) + M\eta + k] \\ &\subseteq D \oplus B_\epsilon. \end{aligned} \quad (23)$$

If $k > 0$ we may write $[G(u) \geq a(1 - \eta) + M\eta + k]$ instead of $[G(u) > a(1 - \eta) + M\eta + k]$. If $G(x)$ has

compact support in B_ϵ , then we may take $\eta = 0$ and, if k satisfies (22), we have

$$\begin{aligned} D \oplus B_\epsilon &\subseteq [G(u) \geq b] \subseteq [G(u) > a + k] \\ &\subseteq D \oplus B_\epsilon. \end{aligned}$$

The value of k may help to maintain separated two level sets so that the quantization step does not destroy them.

Proof: The first inclusion in (23) is a consequence of Lemma 2. The second inclusion follows from (22). Observe that

$$\begin{aligned} [G(u) > a(1 - \eta) + M\eta + k] \\ \subseteq [G(u) > a(1 - \eta) + M\eta] \end{aligned}$$

Finally, the last inclusion in (23) follows from the above observation and Lemma 2. Our last remark follows from the observation that

$$\begin{aligned} [G(u) \geq a(1 - \eta) + M\eta + k] \\ \subseteq [G(u) > a(1 - \eta) + M\eta] \end{aligned}$$

when $k > 0$. □

Practical Consequences. If a level set X is associated with a jump of sufficient size, then after convolution with a kernel of size ϵ , a level set of $G(u)$ will be located at a Hausdorff distance ϵ of X . To get a clearer idea let us illustrate it with a numerical example. We recall that the pixel spacing is $0.5r_0 = \frac{1}{2}\epsilon$. Thus ϵ is interpreted as a two pixel distance. Assume that we do not want to destroy level sets which have a superliminal contrast. Then, assuming $M = 255$, we shall take $b - a = 15$, $k = 1$ (All are standard values in digital processing devices). If we compute $\eta^* = \eta_{15,1} = \frac{b-a-k}{M+b-a} = \frac{14}{270} = 0.0518$. Then we need to choose ϵ such that

$$\int_{\mathbb{R}^2 \setminus B_\epsilon} G(x) dx = 0.0518$$

We recall that $G(x) = (2 \frac{J_1(\pi \frac{r}{r_0})}{\pi \frac{r}{r_0}})^2$ where $r = |x|$. This amounts to 5 pixels as our best ϵ above. Assume $b - a = 15$, $k = 5$, then $\eta = \frac{b-a-k}{M+b-a} = \frac{10}{270} = 0.037$. In the worst case, the level set may have displaced up to say 6 pixels. Finally, assume $b - a = 10$, $k = 2$, then $\eta = \frac{b-a-k}{M+b-a} = \frac{8}{265} = 0.03$. This amounts to around 8 pixels in the worst case.

If $b - a = 30$, $k = 0$, $\eta^* = \eta_{30,0} = \frac{b-a-k}{M+b-a} = \frac{30}{285} = 0.105263157$ we obtain $\epsilon = 3, 5$ pixels. If $b - a = 50$, $k = 0$, $\eta^* = \eta_{50,0} = \frac{b-a-k}{M+b-a} = \frac{50}{305} = 0.163934426$. We almost get to $\epsilon = 2$ pixels.

Let us finally see the effect of the scanning operator.

Lemma 3. *Let u be an image. We assume that $[u \geq \lambda]$ is a constant set D for all $\lambda \in [a, b]$. Then*

$$\begin{aligned} D \ominus Q &\subseteq [A_Q(u) \geq b] \\ &\subseteq [A_Q(u) > a] \subseteq D \oplus Q, \end{aligned} \quad (24)$$

i.e., the level set is displaced at most one pixel by the scanning process.

Proof: Let d be the size of the pixel, i.e., the radius of the square representing the pixel, x be such that $d(x, \mathbb{R}^2 \setminus [u \geq b]) \geq d$. Then

$$A_Q(u)(x) = \frac{1}{\text{Area}(Q)} \int_{x+Q} u(y) dy \geq b \quad (25)$$

Hence $D \ominus Q \subseteq [A_Q(u) \geq b]$. Now if $d(x, D) \geq d$, then

$$A_Q(u)(x) = \frac{1}{\text{Area}(Q)} \int_{x+Q} u(y) dy \leq a. \quad (26)$$

It follows that $[A_Q(u) > a] \subseteq D \oplus Q$. \square

Conclusion. We see from the former Lemma that if an imaging system only consists of a scanning process followed by sampling, then displacement of level lines will be of at most two pixels on both sides of physical ‘edges’. Corollary 1 predicts a larger displacement (up to 8 pixels in the worst case) for optimal imaging systems like astronomic observation devices. Now, returning to images generated by CCD cameras of the today’s technology or scanners, it is easy to check that the ratio between optimal pixel spacing (from the optical viewpoint) and actual pixel spacing is more than 10 (this is even the case for earth observation satellites, like SPOT). Thus it is expected that each ‘edge’ in the image generates about four or five level lines at a one pixel distance from each other. In other words, the pixel displacement predicted by Corollary 1, though existing, is negligible as a displacement factor for all purposes digital imaging systems. This is easily checked in ALL topographic maps displayed here. In fact, a wider width of ‘edges’ in terms of number of level lines is only observed where the image is defocused. The defocussing

can be evaluated by Lemma 3 again, since the defocus kernel is compactly supported, in general some disk or square.

5.2. Digitization of Junctions

We must be able to define the notion of analog and discrete Junction so that the digitization process applied to an ‘analog Junction’ creates a ‘discrete Junction’. We shall assume that both the convolution kernel and the scanning kernel have size ϵ , i.e., we assume that $Q \subseteq B(x, \epsilon)$.

Definition 8. Let $\delta, \rho, R > 0$. Let $u: \Omega \rightarrow \mathbb{R}$ be a bounded measurable function. We say that a point $p \in \Omega$ is an analog Junction (at resolutions given by $\delta, R, \epsilon, \rho > 0$) if

- (i) it is locally stable in the following sense: there exist real numbers $\alpha(p), \beta(p)$ with $\alpha(p) \leq \beta(p) - 2\delta$ and connected components $cc([u < \alpha(p)])$, $cc([\alpha(p) + \delta \leq u < \beta(p) - \delta])$, $cc([\beta(p) \leq u])$ of the sets $[u < \alpha(p)]$, $[\alpha(p) + \delta \leq u < \beta(p) - \delta]$, $[\beta(p) \leq u]$ such that

$$(cc([u < \alpha(p)]) \ominus B_{3\epsilon}) \cap B(p, R) \neq \emptyset$$

$$(cc([\alpha(p) + \delta \leq u < \beta(p) - \delta]) \ominus B_{3\epsilon})$$

$$\cap B(p, R) \neq \emptyset$$

$$(cc([\beta(p) \leq u]) \ominus B_{3\epsilon}) \cap B(p, R) \neq \emptyset$$

- (ii) the sets $cc([u < \alpha(p)]) \ominus B_{3\epsilon}$, $cc([\alpha(p) + \delta \leq u < \beta(p) - \delta]) \ominus B_{3\epsilon}$ and $cc([\beta(p) \leq u]) \ominus B_{3\epsilon}$ are connected by arcs and have an area $\geq \rho$.

Definition 9. Let u be an image and let U be its digital version. We say that there is a discrete Junction (at level of resolution $\delta_1, \rho_1, R > 0$) at $p \in \mathbb{Z}^2$ if there exist real numbers $\alpha_1(p), \beta_1(p)$ with $\alpha_1(p) \leq \beta_1(p) - \delta_1$ and connected components $cc([U < \alpha_1(p)])$, $cc([\alpha_1(p) \leq U < \beta_1(p)])$, $cc([\beta_1(p) \leq U])$ of the sets $[U < \alpha_1(p)]$, $[\alpha_1(p) \leq U < \beta_1(p)]$, $[\beta_1(p) \leq U]$ with area $\geq \rho_1$ such that

$$cc([U < \alpha_1(p)]) \cap B(p, R) \neq \emptyset$$

$$cc([\alpha_1(p) \leq U < \beta_1(p)]) \cap B(p, R) \neq \emptyset$$

$$cc([\beta_1(p) \leq U]) \cap B(p, R) \neq \emptyset$$

Remark. The conditions defining analog and discrete Junctions require some comments. In the definition of analog Junction we assume that 'three objects' arrive at a point p so that the point is a multiple singularity. Moreover, in a neighborhood of the junction, the objects have some interior. This is required if we want to find a trace of the set near the point p after digitization (convolution with a kernel of size or 'aperture' ϵ). Our assumptions are related to the notion of regular model which in the context of mathematical morphology guarantees that the discrete version of a connected set belonging to the regular model will remain a digital connected set ((Serra, 1982), Theorem VII.2, p. 216).

Lemma 4. *Let p be an analog Junction on a continuous image $u: \Omega \rightarrow [0, M]$ at resolutions given by $\delta, R, \epsilon, \rho > 0$. Let U be a digitization of u . Assume that $\frac{2M\eta}{1-\eta} \leq \delta$, where η is given by (12). Then there exists a digital junction at p , possibly at a different level of resolution.*

Proof: If $x \in [u < \alpha(p)] \ominus B_\epsilon$, then $B(x, \epsilon) \subseteq [u < \alpha(p)]$, hence

$$\begin{aligned} \int_{\mathbb{R}^2} G(x-y)u(y)dy &= \int_{B(x,\epsilon)} G(x-y)u(y)dy \\ &+ \int_{\mathbb{R}^2 \setminus B(x,\epsilon)} G(x-y)u(y)dy \\ &< \alpha(p)(1-\eta) + M\eta, \end{aligned}$$

If $x \in [\alpha(p) + \delta \leq u < \beta(p) - \delta] \ominus B_\epsilon$, then

$$\int_{\mathbb{R}^2} G(x-y)u(y)dy \geq (\alpha(p) + \delta)(1-\eta) - M\eta.$$

and

$$\int_{\mathbb{R}^2} G(x-y)u(y)dy < (\beta(p) - \delta)(1-\eta) + M\eta.$$

If $x \in [\beta(p) \leq u] \ominus B_\epsilon$ then

$$\int_{\mathbb{R}^2} G(x-y)u(y)dy \geq \beta(p)(1-\eta) - M\eta$$

Since $\frac{2M\eta}{1-\eta} \leq \delta$, we have that $\alpha(p)(1-\eta) + M\eta \leq (\alpha(p) + \delta)(1-\eta) - M\eta$ and $(\beta(p) - \delta)(1-\eta) + M\eta < \beta(p)(1-\eta) - M\eta$. Let $\alpha_1(p) = \alpha(p)(1-\eta) + M\eta$, $\beta_1(p) = \beta(p)(1-\eta) - M\eta$, $\alpha_2(p) = (\alpha(p) + \delta)(1-\eta) - M\eta$, $\beta_2(p) = (\beta(p) - \delta)(1-\eta) + M\eta$. Notice

we may take $\delta_1 \geq \delta$. From the above inequalities, we deduce

$$\begin{aligned} [u < \alpha(p)] \ominus B_\epsilon &\subseteq [G(u) < \alpha_1(p)] \\ [\alpha(p) + \delta \leq u < \beta(p) - \delta] \ominus B_\epsilon &\subseteq [\alpha_2(p) \leq G(u) < \beta_2(p)] \\ [\beta(p) \leq u] \ominus B_\epsilon &\subseteq [\beta_1(p) \leq G(u)] \end{aligned}$$

Arguing for the first of these level sets, we have that

$$[u < \alpha(p)] \ominus B_{2\epsilon} \subseteq [U < \alpha_1(p)], \quad (27)$$

a priori also

$$[u < \alpha(p)] \ominus B_{3\epsilon} \subseteq [U < \alpha_1(p)]. \quad (28)$$

Now,

$$cc([u < \alpha(p)]) \ominus B_{3\epsilon} \subseteq cc([U < \alpha_1(p)]) \ominus B_{3\epsilon} \quad (29)$$

and we conclude that $cc([U < \alpha_1(p)])$ has an area $\geq \rho$. Similarly for the other two sets. Concerning the connectedness assertion, let $x, y \in cc([u < \alpha(p)]) \ominus B_{3\epsilon}$. Then there exists a curve $\Gamma \subseteq cc([u < \alpha(p)]) \ominus B_{3\epsilon}$ joining x and y . Let us denote by Q a generic pixel, i.e., a square in \mathbb{R}^2 which we shall consider closed in the argument below. We shall identify, by notation, Q with its corresponding sampling point by the Dirac comb. Let $\tilde{\Gamma} = \{Q: Q \cap \Gamma \neq \emptyset\}$. Then $\tilde{\Gamma}$ is connected (4-connected). Let $Q \in \tilde{\Gamma}$. Since the diameter of the pixel is less than ϵ we have that

$$\begin{aligned} Q &\subseteq \Gamma + B(0, 2\epsilon) \subseteq cc([u < \alpha(p)]) \ominus B_\epsilon \\ &\subseteq [G(u) < \alpha_1(p)]. \end{aligned}$$

It follows that $A_Q G(u) < \alpha_1(p)$ on Q . Hence $Q \in [U < \alpha_1(p)]$. Therefore $\tilde{\Gamma} \subseteq [U < \alpha_1(p)]$. We have shown that the set $[U < \alpha_1(p)]$ contains an arcwise-connected subset $cc([u < \alpha(p)]) \ominus B_{3\epsilon}$ of area $\geq \rho$ which, according to (i) intersects $B(p, R)$. Thus $cc([U < \alpha_1(p)]) \cap B(p, R) \neq \emptyset$. A similar result holds for the other two sets. \square

Remark. In the same line of argument as the conclusions we derived for level sets, if the scanning dominates the image formation process, we can expect a displacement of about two pixels on the location of the digital junction with respect to the position of the analog one.

5.3. Phenomenological Interpretation of the Topographic Map

Since the image formation, either continuous or digital, may include an *unknown and non recoverable local contrast change*, we have reduced the image to its parts invariant with respect to contrast changes, the connected components of the level sets of the image. (This invariance requirement was first observed by Wertheimer (1923) who argued that the grey levels in an image are not physically observable.) For digital images (or for continuous ones, if we assume an adequate functional model) the level sets may be described by their boundaries which we called level curves. Thus, for computational purposes, the topographic map of an image may be described by the family of its level curves. Let us discuss on an example how the level lines structure reveals the object occlusion structure.

Figures 3–7 is an elementary example of image generated by occlusion. A grey disk is partly occluded by a darker square (a). In (b) we display a perspective

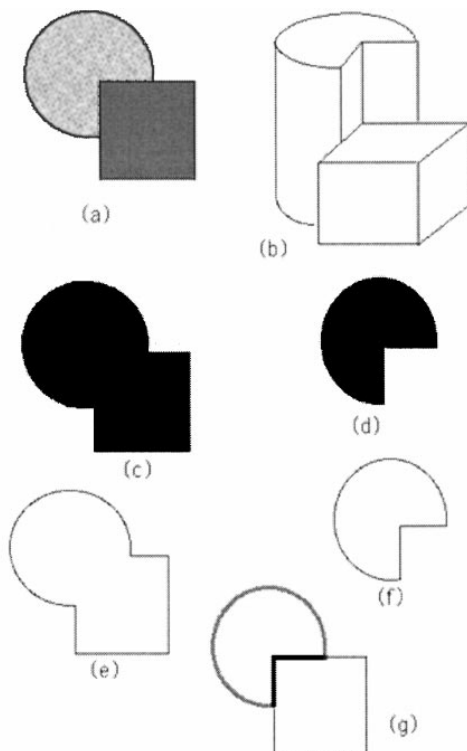


Figure 3. An elementary example of image generated by occlusion.



Image 4.1



Image 4.2

Figure 4. Choice of the parameters. Image 4.1 displays the result of the Junction Detection Algorithm applied to Image 2.2 with area threshold $n = 40$ and grey level threshold $b = 2$ with (in white) small “T”s indicating locations of detected junctions. Image 4.2 displays the same experiment but using an area threshold $n = 100$. We can compare these two results on the same image and we can see the effects on the number of junctions found.

view of the image graph. In (c) and (d) we see two of the four distinct level sets of the image, the other ones being the empty set and the whole plane. It is easily seen that none of the level sets (c) and (d) corresponds to physical objects in the image. Indeed, one of them results from their union and the other one from their set difference. The same thing is true for the level lines (e) and (f): they appear as the result of some “cut and paste” process applied to the level lines of the original objects. Following Kanizsa, we define significant parts

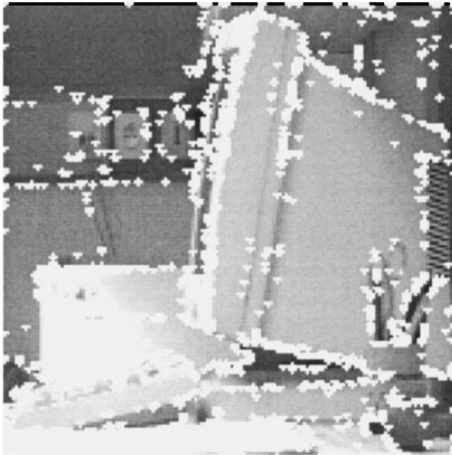


Image 5.1

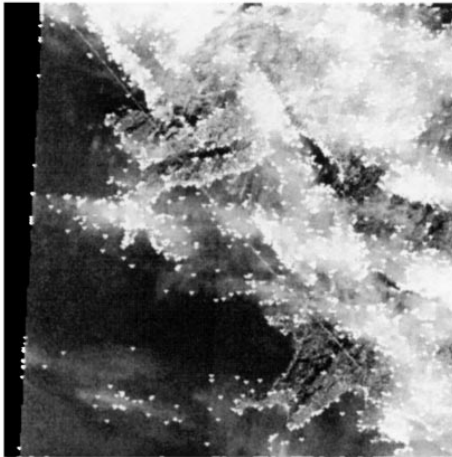


Image 5.2

Figure 5. Examples of junctions. Image 5.1 is the result of the application of the Junction Detection Algorithm with an area threshold $n = 40$ and grey level threshold $b = 2$. The same parameters are used for SPOT Image 5.2.

of images as the result of a segmentation of level lines by T-junctions. The level lines (e) and (f) represent two level lines at two different levels and in (g) we have superposed them in order to put in evidence how they are organized with respect to each other and the resulting T-junctions. We have displayed one of them as a thin line, the other one as a bold line and the common part in grey.

Remark. We shall not go into the classification of Junctions (as T , Y , X , τ , \dots -junctions). For a more detailed discussion we refer to (Caselles et al., 1995).

Let us summarize the main invariance argument.

Invariance Argument

- Since the image formation may include an unknown and non recoverable contrast change: We can reduce the image to its parts invariant with respect to contrast changes, that is, the level lines.
- Since, every time we observe two level lines (or more) joining at a point, this can be the result of an occlusion or of a shadowing, we must break the level lines at this point: indeed, the branches of level lines arriving at a junction are likely to be parts of different visual objects (real objects or shadows). As a consequence, every junction is a possible cue to occlusion or shadowing.

This Invariance Argument needs absolutely no assumption about the physical objects, but only on the “final” part of image generation by contrast changes, occlusions and shadowing. The conclusion of Invariance Argument coincides with what is stated by phenomenology (Kanizsa, 1979, 1991). Indeed, Gaetano Kanizsa proved the main structuring role of junctions (T and X-junctions) in our interpretation of images.

6. Computation and Visualization of the Topographic Map

6.1. Computation of Level Lines and Junctions

In this section, we discuss how level lines and junctions can be computed in digital images and we present experimental results.

In a digital image, the level sets are computed by simple thresholding. A level set $\{u(\mathbf{x}) \geq \lambda\}$ can be immediately displayed in white on black background. In the today’s technology, $\lambda = 0, 1, \dots, 255$, so that we can associate with an image 255 level sets. The Jordan curves limiting the level sets are easily computed by a straightforward contour following algorithm, which yields chains of vertical and horizontal segments limiting the pixels. In the numerical experiments, these chains are represented as chains of pixels by simply inserting “boundary pixels” between the actual image pixels.

According to Definition 9, in the discrete framework, we define “junctions” in general as every point of the image plane where two level lines (with different levels) meet (in a neighborhood of the point). In the experiments below, we take into account junctions if and



Image 6.1

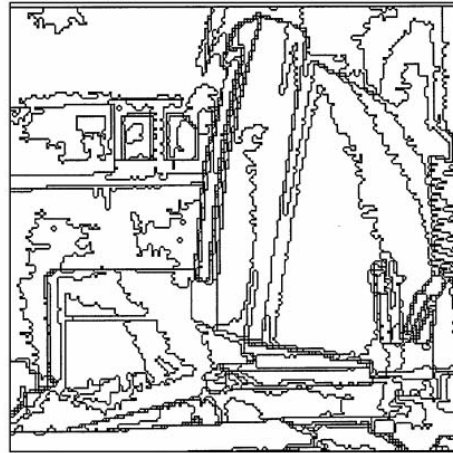


Image 6.2



Image 6.3



Image 6.4



Image 6.5



Image 6.6

Figure 6. Image 6.1 is Image 2.1 in which we have removed all connected components whose area is less than 80 pixels. Image 6.2 displays the level lines of Image 6.1 which are multiples of 20. Image 6.3 is the original image and Image 6.4 shows the Image 6.3 after removing all connected components of area less than 100 pixels. Image 6.5 and Image 6.6 display the level lines of Image 6.3 and Image 6.4, respectively, which are multiples of 30.

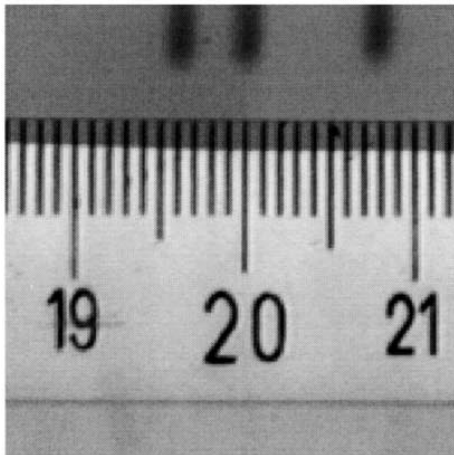


Image 7.1

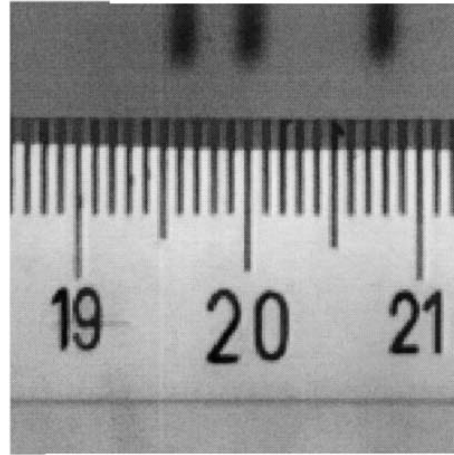


Image 7.2

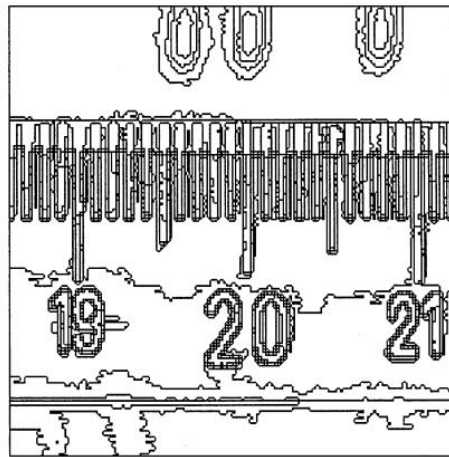


Image 7.3



Image 7.4

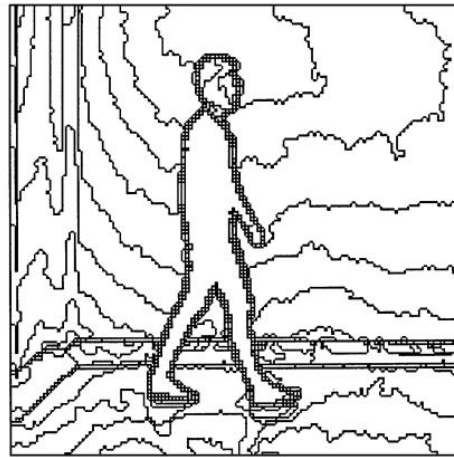


Image 7.5

Figure 7. Image 7.1 is the original image and in Image 7.2 is Image 7.1 after removing all connected components whose area is less than 80 pixels. Image 7.3 shows the level lines of Image 7.2 which are multiples of 20. Image 7.4 is Image 2.2 after removing all connected components of area less than 40 pixels. Image 7.5 displays the level lines of Image 7.4 which are multiples of 10. We note that we can compare this last image with Image 2.5 which gives us the level lines multiples of 10 for the original image.

only if the area of the occulting object, the apparent area of the occulted object and the area of background are large enough.

Discrete Junction Detection Algorithm

- Fix an area threshold n (in practice, $n = 40$ pixels seems sufficient to eliminate junctions due to sampling effects) and a grey level threshold b (in practice: $b = 2$ is sufficient to avoid grey level quantization effects). These values are more optimistic than the ones computed in a ‘worst case’ in Section 5.2.
- At every point \mathbf{x} where two level lines meet: define $\lambda_0 < \mu_0$ the minimum and maximum value of u in the neighboring pixels of \mathbf{x} .
- We denote by L_λ the connected component of \mathbf{x} in the set $\{\mathbf{y}, u(\mathbf{y}) \leq \lambda\}$ and by M_μ the connected component of \mathbf{x} in the set $\{\mathbf{y}, u(\mathbf{y}) \geq \mu\}$. Find the smallest $\lambda \geq \lambda_0$ such that the area of L_λ is larger than n . Call this value λ_1 . Find the largest μ , $\lambda_1 \leq \mu \leq \mu_0$, such that the area of M_μ is larger than n . We call this value μ_1 . If $\mu_1 - \lambda_1 \geq 2b$, and if the set $\{\mathbf{y}, \mu_1 - b \geq u(\mathbf{y}) \geq \lambda_1 + b\}$ has a connected component containing \mathbf{x} with area larger than n , then retain \mathbf{x} as a valid junction. In Fig. 4 and 5, we display the computation of junctions on different images.

We thank the anonymous second referee for the following remark: “The discrete junction algorithm only appears to work when there is a variation in background contrast; this induces a ‘T’ junction between the level lines of the background and the level lines bounding the foreground object; when there is no background variation, there is no junction (according to our definition) and nothing is signaled by our algorithm.” This observation is quite true. In fact, the boundary of the foreground object will have T-junctions in the inside if it is well-contrasted itself and T-junctions on the outside if the background has some contrast. Thus, and although we have seen no instance of it in experiments, an occluding boundary without T-junctions is possible if both foreground and background are strictly constant in grey level.

6.2. Visualisation of the Topographic Map

In this section, we discuss several strategies for visual inspection of the topographic map of a digital image. Clearly, we can see on a screen all level lines of a dig-

ital image by simply zooming the image by a factor 2. This method, however, yields in a good quality image a dense set of lines, so that the structure of the topographic map is too rich to be apparent. Thus, we propose to define strategies for partial, but structured presentation of the topographic map. In contrast with edge maps, to a simplified topographic map is associated a simplified image, so that we can check by visual inspection whether the simplification is not excessive. The main objective of simplifying the topographic map for visual inspection is to single out basic objects, that is, level lines and junctions.

6.2.1. Removal of Small Connected Components.

As a first tool, related to denoising, permitting a good visualization of the topographic map, one can apply the Vincent-Serra algorithm (Vincent, 1993). This contrast invariant algorithm removes all connected extremal regions of the image whose area is less than a fixed number of pixels. This can also be formalized in the Matheron theory as an opening with all connected sets with area less than a threshold, followed by a closing with the same set of structuring elements (see (Masnou and Morel, 1997, 1998a)). As a consequence of this operation, it can be checked in experiments that the topographic map becomes readable, a typical area threshold being between 10 and 30 according to the image size.

6.2.2. Quantization. Another way to make the topographic map readable is to take advantage of the redundancy of the topographic map, particularly on edges, where level lines accumulate. Presenting all level lines with levels multiples of a fixed amount, say 10, will preserve all edges whose contrast is larger than 10. It must be emphasized, however, that we do not pretend that the removed information in the above processes is irrelevant. We simply take advantage of the possibility offered by the topographic representation of a partial, coherent view of the image structure.

Figure 6 and 7 show the result to apply these strategies for the visualization of the topographic map.

6.3. Conclusions

We have shown that a basic structure of an image u invariant to local contrast changes, is given by its topographic map. Its ‘atoms’ are the junctions and the pieces of level lines joining them.

The topographic map has several structural properties, not true for other image descriptions:

1. It contains all the image information, with an obvious reconstruction algorithm, provided we keep the level and orientation of each level line.
2. It needs no scale space, that is, no additional scale parameter. By this, we mean that level lines are, like edges attend to be, global structures and require no parameter for their computations. If we intend to simplify the image, in the scale space sense, that is the removal of small details, this can be performed, as indicated in Section 6, by removing small level lines, in which case a scale parameter is introduced. The need for a more classical scale space can arise when we wish to smooth each level line as well. This is possible by using curve scale spaces (Kimia et al., 1992; Alvarez et al., 1993; Sapiro and Tannenbaum, 1993, 1994), who use variants of the Osher-Sethian curve evolution computational theory.) From the viewpoint adopted in (Caselles et al., 1993), and further on in (Malladi et al., 1995), image scale space is performed separately on each level line of the image.
3. In contrast with “edges”, level lines need no connectedness algorithm to be computed: they are immediately connected curves. The question must be raised, of how the topographic map can help to get back to the physical structure of underlying objects. As far as shape recognition is concerned, it must be emphasised that pieces of level lines between junctions perform an easy to compute grouping which can be used for shape recognition, in the same way as edges are.
4. Its structure is preserved under standard digitization processes.

7. Discussion

The mathematical discussion of the stability of level lines and junctions performed in Sections 5.1 and 5.2 by no means pretends to lead to a detection theory. It only proves that under certain conditions of contrast and size of the regions in the analogous image, the level lines and junctions will be preserved in the digitization process. Now, we do not exclude the creation of spurious level lines and junctions due to the digitization process.

As noticed by the second, anonymous reviewer, the definition of junction corresponds to the conjunction of multiple conditions, some of which are introduced to guarantee the existence of intensity relationships (the α 's and β 's) that persist over a neighborhood given

some erosion. This is analogous, in a sense, to the more recent attempts to define nonlinear edge detectors (see e.g. (Iverson and Zucker, 1995)).

Between the first submission of this paper and the final revision, three years have transpired, and this has the main advantage of having given time to several technological developments. It had to be demonstrated that the local contrast invariant structure given by the topographic map can be used in applications. The first obvious idea has been to use it for the comparison of images taken at different times and under different illumination or weather conditions. This is performed in (Ballester et al., 1998) on satellite images. The idea is to compare all connected components of level sets in both images and, more generally, all “sections”, that is, connected components of bilevel sets $[\lambda \leq u \leq \mu]$, $\lambda, \mu \in \mathbb{R}$. Thanks to this algorithm, images of the same scene with very different radiometry can be compared and it has been experimentally shown that they have many parts of their topographic maps in common. In addition, the complete description given by a topographic map permitting reconstruction, the comparison algorithm also yields an intersection image, that is, an image having roughly for topographic map the intersection of topographic maps of both compared images. A further extension of this idea is performed in P. Monasse, who uses Jordan curves of the topographic map of two views in order to perform registration. P. Monasse and F. Guichard have proposed a Fast Level Set Transform in (Monasse and Guichard, 1998), which defines the topographic map as a tree of Jordan curves. All operations mentioned above (intersection, registration, Vincent-Serra filters, etc.) can be performed in “real time” thanks to the FLST. Simon Masnou uses the topographic map in order to perform disocclusion, that is, a reconnection of level lines arriving to junctions bounding a spot in the image (Masnou and Morel, 1998a). In a forthcoming paper, Jacques Froment uses explicitly the level-lines-junctions as described in this paper to propose a structured compression algorithm which selects the most significant part of the topographic map and also uses the possibility offered of reconstructing an image from a part of a topographic map (Froment, 1998).

Appendix: The Upper Topographic Map

During the proof of Theorem 5 we shall need the notion of maximal monotone graph. A monotone graph is a set-valued function $\mathbb{R} \rightarrow \mathcal{P}(\mathbb{R})$ such that for every $\lambda \in \mathbb{R}$, $G(\lambda) = [g_*(\lambda), g^*(\lambda)]$ is a closed interval

and $\lambda > \mu$ implies $g_*(\lambda) \geq g^*(\mu)$. Here g_* (resp. g^*) is a non-decreasing lower semicontinuous (resp. upper semicontinuous) function from \mathbb{R} to \mathbb{R} . We say that a monotone graph G is continuous or maximal monotone if, in addition, the range of G has no gaps, that is, $\cup_\lambda G(\lambda)$ is an interval of \mathbb{R} . Note that G can be recovered from g^* (resp. g_*) by setting

$$g_*(\lambda) = \sup\{g^*(\mu): \mu < \lambda\} \quad (30)$$

in the first case and

$$g^*(\lambda) = \inf\{g_*(\mu): \mu > \lambda\}$$

in the second case.

Condition (H1) in Definition 6 is justified by the following result.

Lemma 5. *Let $f: \Omega \times \mathbb{R} \rightarrow \mathbb{R}$ be a function such that*

- (i) $f(x, \lambda)$ is increasing upper semicontinuous as a function of λ for all $x \in \Omega$.
- (ii) $f(x, \lambda)$ is measurable as a function of x for each $\lambda \in \mathbb{R}$.

Then for any bounded measurable function $u: \Omega \rightarrow [a, b]$ the function $v(x) = f(x, u(x))$ is also measurable.

Proof: Recall that a function $v(x)$ is measurable if and only if for every $\lambda \in \mathbb{R}$ the level sets $[x: v(x) \leq \lambda]$ are Lebesgue measurable. Recall also that countable unions and intersections of measurable sets are measurable. Now $[x: v(x) \leq \lambda] = [x: f(x, u(x)) \leq \lambda]$. Let us choose a dense sequence $(b_k)_{k \in \mathbb{N}}$ in \mathbb{R} . Since f is upper semicontinuous as a function of λ for all $x \in \Omega$, we have that $f(x, r) \leq \lambda$ if and only if for all $n \in \mathbb{N}$, there exist $k \in \mathbb{N}$ such that $r \leq b_k$ and $f(x, b_k) \leq \lambda + \frac{1}{n}$. Thus, $[x: v(x) \leq \lambda] = [x: \forall n, \exists k, b_k \geq u(x) \text{ and } f(x, b_k) \leq \lambda + \frac{1}{n}] = \cap_n \cup_k ([x: u(x) \leq b_k] \cap [x: f(x, b_k) \leq \lambda + \frac{1}{n}])$. Hence v is measurable. \square

Proof of Proposition 1:

- (i) If $x \in X_\lambda u$, $\lambda \in \mathbb{R}$, then $u(x) \geq \lambda$ and $v(x) = h^+(x, u(x)) \geq h^{1+}(x, \lambda)$, i.e., $x \in X_{h^+(x, \lambda)} v$. Conversely, if $x \in X_{h^+(x, \lambda)} v$, then $h^+(x, u(x)) \geq h^+(x, \lambda)$. By (H2), this implies that $u(x) \geq \lambda$, i.e., $x \in X_\lambda u$. It is also easy to see that $v(x) = \sup\{h^+(x, \lambda'): x \in X_{\lambda'} u\}$.

- (ii) Define

$$h^{-*}(x, \lambda) = \inf_{\mu > \lambda} h^-(x, \mu)$$

By (H2), $h^{-*}: \Omega \times \mathbb{R} \rightarrow \mathbb{R}$. Since

$$h^{-*}(x, \lambda) = \inf_{\mu_n \searrow \lambda} h^-(x, \mu_n),$$

$h^{-*}(x, \lambda)$ is measurable in x for all $\lambda \in \mathbb{R}$. We know also that $h^{-*}(x, \lambda)$ is an increasing upper semicontinuous function (hence, continuous on the right) of λ for all x . By Lemma 5, we know that $h^{-*}(x, u(x))$ is a measurable function of x . Now, using (H2),

$$h^{-*}(x, u(x)) = \inf_{\mu > u(x)} h^-(x, \mu) = h^+(x, u(x)).$$

We conclude that $v(x) = h^+(x, u(x))$ is measurable.

- (iii) If $y \in \Gamma' = cc([u \geq \lambda], x)$, then, by (H3), $h^+(x, \lambda) = h^+(y, \lambda) \leq h^+(x, u(y)) = v(y)$. Since $\mu = h^+(x, \lambda)$, $v(y) \geq \mu$. Hence, $\Gamma' \subseteq [v \geq \mu]$. Since Γ' is connected and contains x , it follows that $\Gamma' \subseteq cc([v \geq \mu], x) = \Gamma$. Now, if the inclusion were strict, then for some $z \in cc([v \geq \mu], x)$, $u(z) < \lambda$. If $h^+(x, \lambda) \in h(x, \lambda)$, then, using (H4), $h(x, \lambda) = h(z, \lambda)$. If $h^+(x, \lambda) \notin h(x, \lambda)$, then there exists some $\mu' < \mu$ such that $\mu' \in h(x, \lambda)$ and $z \in cc([v \geq \mu'], x)$. Again, by (H4), $h(x, \lambda) = h(z, \lambda)$. In any case, $\mu = h^+(x, \lambda) = h^+(z, \lambda)$. On the other hand, by (H2), $h^+(z, \lambda) > h^+(z, u(z)) = v(z) \geq \mu$, a contradiction.
- (iv) Let X be a connected component of $[u \geq \lambda]$ and let $x \in X$. Then, using (iii), $X = cc([u \geq \lambda], x) = cc([v \geq \mu], x)$ where $\mu = h^+(x, \lambda)$. Conversely, let $Y = cc([v \geq \mu], x)$, $\mu \in \mathbb{R}$. If v takes values in $[c, d]$, without loss of generality, we may assume that $\mu \in [c, d]$. Let $\lambda \in \mathbb{R}$ such that $\mu \in h(x, \lambda)$. We know that $cc([u \geq \lambda], x) = cc([v \geq h^+(x, \lambda)], x) \subseteq cc([v \geq \mu], x)$. If the inclusion is strict, then $u(y) < \lambda$ for some $y \in cc([v \geq \mu], x)$. Since, by (H4), $h(x, \lambda) = h(y, \lambda)$, then $\mu \in h(y, \lambda)$. Using (H2), we may write

$$\mu \leq v(y) = h^+(y, u(y)) = h^-(y, \lambda) \leq \mu.$$

Hence, $\mu = h^+(y, u(y))$. Now, using (iii), we

have

$$\begin{aligned} cc([v \geq \mu], x) &= cc([v \geq h^+(y, u(y))], y) \\ &= cc([u \geq u(y)], y). \end{aligned}$$

In other words, there is some $\alpha = u(y)$ and some connected component X of X_α such that $X = Y$. \square

Let us prove the converse of Proposition 1 given by Theorem 1.

Theorem 1. *Let $u, v: \mathbb{R}^n \rightarrow \mathbb{R}$ be two bounded measurable functions (images) whose upper level sets have, at most, countably many connected components. Let X_λ , respectively Y_λ , be the families of the level sets of u , respectively v . Suppose that for each connected component X of X_λ there exists μ and a connected component Y of Y_μ such that $X = Y$ and a converse statement with X_λ and Y_μ interchanged. Then there exists a local contrast change $g(x, \lambda)$ such that $v(x) = g^+(x, u(x))$.*

Proof: Suppose that u takes values in $[a, b]$ and v takes values in $[c, d]$. Let $x \in \mathbb{R}^n$ and $\lambda \in \mathbb{R}$. If $a \leq \lambda \leq u(x)$, then $x \in X_\lambda$ and we define the set (nonempty, by assumption)

$$G(x, \lambda) = \{\lambda' \in [c, d]: cc(X_\lambda, x) = cc(Y_{\lambda'}, x)\}.$$

If $\lambda > u(x)$ we define $G(x, \lambda) = [v(x), d + 1]$. If $\lambda < a$, we define $G(x, \lambda) = [c - 1, c]$. Let us prove that G is a monotonous multifunction.

Step 1. $G(x, \lambda)$ is an interval. We may assume that $a \leq \lambda \leq u(x)$. If λ' and λ'' belong to $G(x, \lambda)$, then for every $\lambda' < \mu < \lambda''$, we have

$$\begin{aligned} cc(X_\lambda, x) &= cc(Y_{\lambda'}, x) \subseteq cc(Y_\mu, x) \\ &\subseteq cc(Y_{\lambda''}, x) = cc(X_\lambda, x), \end{aligned}$$

so that $\mu \in G(x, \lambda)$. Consequently, $G(x, \lambda)$ is an interval. Let $g^-(x, \lambda) = \inf\{\mu: \mu \in G(x, \lambda)\}$, $g^+(x, \lambda) = \sup\{\mu: \mu \in G(x, \lambda)\}$. Observe that, when $a \leq \lambda \leq u(x)$, $g^+(x, \lambda) \leq v(x)$.

Step 2. We wish to show that if $\lambda > \mu$, then either $G(x, \lambda) = G(x, \mu)$ or $g^-(x, \lambda) \geq g^+(x, \mu)$. We may assume that $a \leq \mu < \lambda \leq u(x)$. Indeed, since $\lambda > \mu$, we have that $cc(X_\lambda, x) \subseteq cc(X_\mu, x)$ and therefore $cc(Y_{\lambda'}, x) \subseteq cc(Y_{\mu'}, x)$ for every $\lambda' \in G(x, \lambda)$ and $\mu' \in G(x, \mu)$. If

$cc(X_\lambda, x) = cc(X_\mu, x)$, we immediately see from the definition of G that $G(x, \lambda) = G(x, \mu)$. If $cc(X_\lambda, x) \neq cc(X_\mu, x)$, then for every $\lambda' \in G(x, \lambda)$ and $\mu' \in G(x, \mu)$ we have $cc(Y_{\lambda'}, x) \subseteq cc(Y_{\mu'}, x)$ and $cc(Y_{\lambda'}, x) \neq cc(Y_{\mu'}, x)$, so that $\lambda' > \mu'$.

Step 3. Let $x \in \mathbb{R}^n$. We finally show that $G(x, \cdot)$ is onto in the sense that $\cup_\lambda G(x, \lambda) = [c - 1, d + 1]$. Let $\lambda' \in [c - 1, d + 1]$. By definition of G we may assume that $c \leq \lambda' \leq v(x)$. By assumption for every $\lambda' \in [c, v(x)]$ and every connected component of $Y_{\lambda'}$ containing x , $cc(Y_{\lambda'}, x)$, there exists some $\lambda \in \mathbb{R}$ such that $cc(Y_{\lambda'}, x) = cc(X_\lambda, x)$. Thus $\lambda' \in G(x, \lambda)$.

Step 4. By definition of G we have that $g^+(x, u(x)) \leq v(x)$. Now, since

$$\begin{aligned} v(x) &= \sup\{\mu: x \in Y_\mu\} \\ &= \sup\{\mu: \mu \in G(x, \lambda) \quad \lambda \text{ s. t. } x \in X_\lambda\} \\ &= \sup\{g^+(x, \lambda): \lambda \text{ s. t. } x \in cc(X_\lambda, x)\} \\ &\leq g^+(x, \sup\{\lambda: x \in cc(X_\lambda, x)\}), \end{aligned}$$

we have that $v(x) = g^+(x, u(x))$.

We finish the proof with the next Lemma.

Lemma 6. *$G(x, \lambda)$ is a local contrast change of u .*

Proof:

(H1) Let $\lambda \in \mathbb{R}$. Let us prove that the correspondence $x \in \Omega \rightarrow \bar{G}(x, \lambda) =$ the closure of $G(x, \lambda)$ has a measurable graph. Since it is a correspondence whose values are closed sets this is equivalent to prove that $x \in \Omega \rightarrow \bar{G}(\cdot, \lambda)$ is weakly measurable, that is, for any open set O in \mathbb{R} , the set $\{x \in \Omega: \bar{G}(x, \lambda) \cap O \neq \emptyset\}$ is measurable ((Aliprantis, 1994), chap. 14). It is sufficient to consider the case where O is an interval (α, β) . If $\lambda < a$ this set is obviously measurable. Assume that $\lambda \geq a$. Observe that we may write $\{x \in \Omega: \bar{G}(x, \lambda) \cap O \neq \emptyset\}$ as the union of two sets:

$$\begin{aligned} A &= \{x \in \Omega: u(x) \geq \lambda, \quad \bar{G}(x, \lambda) \cap O \neq \emptyset\} \\ B &= \{x \in \Omega: u(x) < \lambda, \quad \bar{G}(x, \lambda) \cap O \neq \emptyset\}. \end{aligned}$$

Since

$$B = \{x \in \Omega: u(x) < \lambda, \quad [v(x), d + 1] \cap O \neq \emptyset\},$$

it is obviously measurable. If $u(x) \geq \lambda \geq a$, observe that $\tilde{G}(x, \lambda) \cap O \neq \emptyset$ if and only if there exists some $\mu \in O$ such that $cc(X_\lambda, x) = cc(Y_\mu, x)$. Now, if for some $x \in \Omega$, $\tilde{G}(x, \lambda) \cap O \neq \emptyset$, then for all $y \in cc(X_\lambda, x)$ there exists some $\mu \in \mathbb{R}$ (the same as above) such that $cc(X_\lambda, y) = cc(X_\lambda, x) = cc(Y_\mu, x) = cc(Y_\mu, y)$. Thus, for any $x \in \Omega$ we have either

$$cc(X_\lambda, x) \subseteq A$$

or

$$cc(X_\lambda, x) \cap A = \emptyset.$$

We may write

$$A = \cup\{cc(X_\lambda) : \exists \mu \in O \text{ s. t. } cc(X_\lambda) = cc(Y_\mu)\}. \quad (31)$$

Since the connected components of X_λ , being closed in X_λ , are measurable and there are, at most, countably many, it follows that A is a measurable subset of Ω and the multifunction $\tilde{G}(\cdot, \lambda)$ is weakly measurable. According to the measure theoretic analogue of Berge's theorem $g^+(x, \lambda) = \sup\{\mu : \mu \in G(x, \lambda)\} = \sup\{\mu : \mu \in \tilde{G}(x, \lambda)\}$ is a measurable function ((Eatwell et al., 1994), vol. 1, p. 680).

- (H2) If $u(x) < \lambda$, by the definitions above $g^+(x, u(x)) = g^-(x, \lambda) < g^+(x, \lambda)$. Note that $\inf_{x \in \Omega} g^-(x, \lambda) \geq c - 1$ and $\sup_{x \in \Omega} g^+(x, \lambda) \leq d + 1$, for each $\lambda \in \mathbb{R}$.
- (H3) Let $\lambda \in \mathbb{R}$, x, y in the same connected component of $[u \geq \lambda]$. If $\lambda' \in G(x, \lambda)$, then $cc(X_\lambda, x) = cc(Y_{\lambda'}, x)$. Since $y \in cc(X_\lambda, x) = cc(Y_{\lambda'}, x)$ then $cc(X_\lambda, y) = cc(X_\lambda, x) = cc(Y_{\lambda'}, x) = cc(Y_{\lambda'}, y)$. Hence, $\lambda' \in G(y, \lambda)$. Therefore $G(x, \lambda) \subseteq G(y, \lambda)$. The other inequality being proven similarly, it follows that $G(x, \lambda) = G(y, \lambda)$ and, in consequence, $g^+(x, \lambda) = g^+(y, \lambda)$.
- (H4) Assume that $y \in cc([v \geq \mu], x)$ with $\mu \in G(x, \lambda)$, $x, y \in \Omega$, $\lambda \in \mathbb{R}$. Then $cc([v \geq \mu], x) = cc(X_\lambda, x)$. Hence $y \in cc(X_\lambda, x)$. Thus $cc(X_\lambda, x) = cc(X_\lambda, y)$ and $G(x, \lambda) = G(y, \lambda)$ follows. \square
- (H5) If u, v of Theorem 1 are lower semicontinuous functions then almost all upper level sets have, at most, countably many connected components (modulus a null set). The Proof of Theorem 1 can be easily adapted to this context. \square

Acknowledgments

We gratefully acknowledge partial support by DGICYT project, reference PB94-1174, by european project PAVR, reference ERB FMRX-CT96-0036, the TMR European project Viscosity Solutions and their Applications, FMRX-CT98-0234, and Centre National d'Etudes Spatiales (CNES).

References

- Aliprantis, Ch.D. and Border, K.C. 1994. *Infinite Dimensional Analysis*. Springer Verlag.
- Alison Noble, J. 1992. Finding half boundaries and junctions in images. *Image and Vision Computing*, 10(4).
- Alvarez, L., Guichard, F., Lions, P.L., and Morel, J.M. 1993. Axioms and fundamental equations of image processing. *Arch. Rational Mechanics and Anal.* 16(IX):200–257.
- Alvarez, L. and Morales, F. 1994. Affine morphological multiscale analysis of corners and multiple junctions. *International Journal of Computer Vision*, 25(2):95–108.
- Alvarez, L. and Morel, J.M. 1994. Formalization and computational aspects of image analysis. *Acta Numerica*, pp. 1–59.
- Ambrosio, L., Caselles, V., Masnou, S., and Morel, J.M. 1999. *The Connected Components of Sets of Finite Perimeter and Applications to Image Processing*. Preprint SNS, Pisa, Italy.
- Ballester, C., Cubero-Castan, E., Gonzalez, M., and Morel, J.M. 1998. *Contrast Invariant Image Intersection*, preprint.
- Beymer, D.J. 1991. Finding junctions using the image gradient. *Computer Vision and Pattern Recognition*, Lahaiana, Maui, Hawaii, pp. 720–721.
- Brunnström, K., Linderberg, T., and Eklundh, J.O. 1992. Active detection and classification of junctions by foveation with a head-eye system guided by the scale-space primal sketch. Technical Report ISRN KTH/NA/P-91/31, CVAP, Royal Institute of Technology.
- Canny, J.F. 1986. A computational approach to edge detection. *IEEE Transactions on Pattern Analysis and Machine Intelligence*, 8:769–798.
- Caselles, V., Catté, F., Coll, B., and Dibos, F. 1993. A Geometric Model for Edge Detection. *Numerische Mathematik*, 66:1–31.
- Caselles, V., Coll, B., and Morel, J.M. 1995. A Kanizsa programme. Preprint CEREMADE 9539, Univ. Paris-Dauphine.
- Caselles, V., Coll, B., and Morel, J.M. 1997. Scale-space versus topographic map for natural images. In *Scale-space '97. Proc. First Conference on Scale Space*, Utrecht.
- Caselles, V., Lisani, J.L., Morel, J.M., and Sapiro, G. 1997. Shape preserving local histogram modification. Technical Report HPL-97-58.
- Caselles, V., Morel, J.M., and Sbert, C. 1998. An axiomatic approach to image interpolation. Special Issue on PDE's, Geometry Driven Diffusion and Image Processing. *IEEE Transactions on Image Processing*, 7(3):376–386.
- Castleman, K.R. 1996. *Digital Image Processing*. Prentice Hall.
- Choquet, G. 1966. *Topology*, Academic Press: New York.
- Deriche, R. and Blaszkza, T. 1993. Recovering and characterizing image features using an efficient model based approach. *Proc. CVPR*, New York, pp. 530–535.

- Deriche, R. and Giraudon, G. 1993. A computational approach for corner and vertex detection. *International Journal of Computer Vision*, 10(2):101–124.
- Eatwell, J., Milgate, M., and Newman, P. (Eds.). 1994. *The New Palgrave, a Dictionary of Economics, 4 volumes*. The Macmillan Press Limited.
- Evans, L.C. and Gariepy, R. 1992. *Lectures Notes on Measure Theory and Fine Properties of Functions*. CRC Press.
- Fitch, J.P., Coyle, E.C., and Gallagher, N.C. 1985. Threshold decomposition of multi-dimensional ranked order operations. *IEEE Trans. on Circuits and Systems*, 5:445–450.
- Florack, L.M.J. 1993. The syntactical structure of scalar images. Ph.D. Thesis, University of Utrecht, The Netherlands.
- Froment, J. et al. 1997. *MegaWave, Image Processing Environment*, Ceremade, Université Paris-Dauphine.
- Froment, J., *A Functional Analysis Model for Natural Images Permitting Structured Compression*. Preprint 9833, CMCA, ENS Cachan, France.
- Fuchs, W. 1923. Experimentelle Untersuchungen ueber das simultane Hintereinandersehen auf der selben Sehrichtung. *Zeitschrift fuer Psychologie*, 91:154–253.
- Haar Romeny, B.M. ter. 1994. *Geometry-Driven Diffusion in Computer Vision*. Kluwer Academic Publications.
- Haar Romeny, B.M. ter, Florack, L.M.J., Koendering, J.J., and Viergever, M.A. 1991. Invariant third-order properties of isophotes: T-junction detection. In *Proc. Scandinavian Conference on Image Analysis*.
- Haralick, R.M. and Shapiro, L.G. 1992. *Computer and Robot Vision, I*. Addison-Wesley.
- Hecht, E. and Zajac, A. 1986. *Optica*. Addison Wesley Iberoamericana.
- Heitger, F. and von der Heydt, R. 1993. A computational model of neural contour processing: Figure-ground segregation and illusory contours. In *4th Proc. International Conference on Computer Vision*, Berlin, Germany. IEEE Computer Society Press, pp. 32–40.
- Illueca, C. 1995. Influence of contrast of the recognition of defocused letters: A geometrical model. Vision Research.
- Iverson, L.A. and Zucker, S.W. 1995. Logical/linear operators for image curves. *IEEE Trans. Pattern Anal. Machine Intell.* 17(10): 982–996.
- Julesz, B. 1981. Textons, the elements of texture perception, and their interactions. *Nature*, 290(3).
- Julesz, B. 1986. Texton gradients: The texton theory revisited. *Biological Cybernetics*, 54:245–251.
- Kanizsa, G. 1979. *Organization in Vision*. NY, Praeger.
- Kanizsa, G. 1991. *Vedere e pensare*. Il Mulino, Bologna.
- Kimia, B.B., Tannenbaum, A., and Zucker, S.W. 1992. On the evolution of curves via a function of curvature, 1: The classical case. *J. of Math. Analysis and Applications*, 163(2).
- Koenderink, J.J. 1984. The structure of images. *Biological Cybernetics*, 50:363–370.
- Leclerc, Y.G. and Zucker, S.W. 1987. The local structure of Image discontinuities in one dimension. *IEEE Trans. Pattern Anal. Machine Intell.*, 9:4.
- Lindeberg, T. 1994. Junction detection with automatic selection of detection scales and localization scales. In *Proc. First Int. Conf. on Image Processing*, Austin, Texas, vol. 1, pp. 924–928.
- Malik, J. 1987. Interpreting line drawings of curved objects. *Int. J. Comp. Vision*, 1.
- Malladi, R., Sethian J., and Vemuri, B.C. 1995. Shape modelling with front propagation: A level set approach. *IEEE Trans. on Pattern Anal. Machine Intell.*, 17(2):158–175.
- Marr, D. 1981. *Vision*, Freeman and Co.
- Masnou, S. and Morel, J.M. 1997. Restauration d'images et filtres de Yaroslarsky. In *Proc. Workshop GRETSI 97*, Grenoble, France.
- Masnou, S. and Morel, J.M. 1998a. Level lines based disocclusion. In *Proc. Int. Conf. Image Processing, ICIP'98*, Chicago, USA, vol. III, pp. 259–263.
- Masnou, S. and Morel, J.M. 1998b. Image restoration involving connectedness. In *Proc. of Workshop "Digital Image Processing"*, Vienna, Austria 1997, SPIE, vol. 3346.
- Matheron, G. 1975. *Random Sets and Integral Geometry*, John Wiley, NY.
- Monasse, P. and Guichard, F. 1998. Fast computation of a contrast invariant image representation. *Cahiers de l'ENS Cachan*, 9815.
- Morel, J.M. and Solimini, S. 1994. *Variational Methods in Image Processing*. Birkhäuser.
- Nitzberg, M. and Mumford, D. 1990. The 2.1 sketch. In *Proc. of the Third International Conference on Computer Vision*, Osaka.
- Nitzberg, M., Mumford, D., and Shiota, T. 1993. *Filtering, Segmentation and Depth*. Lecture Notes in Computer Science, 662, Springer-Verlag.
- Osher, S. and Sethian, J. 1988. Fronts propagating with curvature dependent speed: Algorithms based on the Hamilton-Jacobi formulation. *J. Comp. Physics*, 79:12–49.
- Rudin, L.I. 1987. Images, numerical analysis of singularities and shock filters. Ph.D. Dissertation, Caltech, Pasadena, CA, n5250:TR.
- Rudin, L.I., Osher, S., and Fatemi, E. 1992. Nonlinear total variation based noise removal algorithms. *Physica D*, 60:259–269.
- Sapiro, G. and Tannenbaum, A. 1993. Affine invariant scale space. *The International Journal of Computer Vision*, 11(1):25–44.
- Sapiro, G. and Tannenbaum, A. 1994. On affine plane curve evolution. *Journal of Functional Analysis*, 119(1):79–120.
- Serra, J. 1982. *Image Analysis and Mathematical Morphology*. Academic Press.
- Vincent, L. 1993. Grayscale area openings and closings, their efficient implementation and applications. In *First Workshop on Mathematical Morphology and its Applications to Signal Processing*, J. Serra and Ph. Salembier (Eds.), Barcelona, Spain, pp. 22–27.
- Wertheimer, M. 1923. Untersuchungen zur Lehre der Gestalt, II. *Psychologische Forschung*, 4:301–350.
- Witkin, A.P. 1983. Scale-space filtering. In *Proc. of IJCAI*, Karlsruhe, pp. 1019–1021.